

# Phyto-mediated Synthesis of Silver Nanoparticles with *Afrohybanthus travancoricus* Leaf Aqueous Extract and Screening of their *in vitro* Antioxidant, Anti-Inflammatory, and Anti-diabetic Activities

Balrajmani Davidson Raja<sup>1</sup>, Devaraj Sathiya Sheela<sup>1</sup>, Elumalai Shanthi Priya<sup>1</sup>, Ammasaikutty Vanitha<sup>2</sup>, Kandasamy Kalimuthu<sup>1</sup>, Periannan Viswanathan<sup>1,\*</sup>

<sup>1</sup>Department of Botany, Government Arts College (Autonomous), Coimbatore, Tamil Nadu, INDIA.

<sup>2</sup>Department of Botany, Namakkal Kavignar Ramalingam Government Arts College for Women, Namakkal, Tamil Nadu, INDIA.

## ABSTRACT

**Aim:** There are many uses for silver nanoparticles in the field of biomedicine due to their exceptional properties. A major application of silver nanoparticles is the increase of antibiotics that are clinically helpful against microbes and drug-resistant bacteria. However, environmentally friendly methods for their synthesis must be developed. **Objectives:** Current study, the major objective of this research is concentrated on to suggest an easy and well-organized biosynthesis of silver nanoparticles by confirmed antioxidant, anti-inflammatory and anti-diabetic activities. The ATSNPs (*Afrohybanthus travancoricus* silver nanoparticles) was biosynthesized with *A. travancoricus* plant like capping and reducing agent. **Materials and Methods:** The ATSNPs aqueous extract were mixed by water extract of 1mM AgNO<sub>3</sub> solution led to appearance of greenish brown to dark brown colour indicates the synthesis of SNPs. The silver nanoparticles were characterized by UV-visible spectroscopy, FT-IR, SEM, XRD, and EDX analysis. Antioxidant assay was tested through DPPH and ABTS<sup>+</sup> assays, anti-inflammatory assay through albumin denaturation and antidiabetic assay by  $\alpha$ -amylase and  $\alpha$ -glucosidase activities. **Results:** A colour change of solution from dark brown to light brown, absorption peak of ATSNPs as 290 to 300 nm in UV-vis spectroscopy. ATSNPs showed 6 intense peaks in FTIR analysis and functional groups like phenols, alcohols, 1° amines, alkynes, aliphatic amines, aromatics, and alkyl halides were identified. In XRD analysis showed 5 intense peaks at 20.8°, 30.3°, 40.1°, 40.9°, 60°. The EDX analysis the presence of Ag at 3 keV and SEM analysis showed the size of ATSNPs ranges between 88  $\mu$ m – 242  $\mu$ m. Antioxidant activity was observed the dose dependent manner in both assays. Anti-inflammatory activity of ATSNPs proved maximum inhibition through egg albumin denaturation. Antidiabetic activity exhibits maximum inhibition percentage of  $\alpha$ -amylase and  $\alpha$ -glucosidase at 10  $\mu$ g/mL. The lowest IC<sub>50</sub> value was noted in  $\alpha$  amylase (170  $\mu$ g/mL) and  $\alpha$  glucosidase (134  $\mu$ g/mL). **Conclusion:** The obtained results recommended that using ATSNPs, it is likely to represented silver nanoparticles with controlled characteristics and important pharmacological activities.

**Keywords:** *Afrohybanthus travancoricus*, Green synthesis, Silver nanoparticles, Antioxidant, Anti-inflammatory, Anti-diabetic activity.

## Correspondence:

**Dr. Periannan Viswanathan**

Assistant Professor, PG and Research  
Department of Botany, Government Arts  
College, Affiliated to Bharathiar University  
Coimbatore-641018, Tamil Nadu, INDIA.  
Email: rpviswanathan68@gmail.com

**Received:** 18-05-2023;

**Revised:** 04-06-2023;

**Accepted:** 23-06-2023.

## INTRODUCTION

Due to its distinctive and alluring physicochemical properties, nanotechnology is one of the most fascinating and difficult research areas in pharmacology, water treatment, modern materials science, and biomedical engineering.<sup>[1-3]</sup> Metal nanoparticles have a wide range of uses, including their antioxidant

potency, anti-microbial activity against human pathogens, and use in food products, anti-inflammatory properties in cosmetics, and cancer treatment and diagnosis.<sup>[4]</sup>

The preparation of silver nanoparticles has been studied using a variety of methods recently, including chemical and electrochemical ones (SNPs). However, most methods have problems with the purification stage because the by-products or chemicals used are dangerous and require a lot of energy to prepare.<sup>[5]</sup> To make nanoparticles, a variety of materials are employed, including metals, silicates, non-oxide ceramics, metal oxide ceramics, and metals.



DOI: 10.5530/pres.15.4.079

### Copyright Information :

Copyright Author (s) 2023 Distributed under  
Creative Commons CC-BY 4.0



Publishing Partner : EManuscript Tech. [www.emanuscript.in]

The reduction of nanoparticles using chemical, photochemical, or electrochemical processes is currently the most popular technique.<sup>[6]</sup> Researchers frequently face difficulties in managed the size and shape of nanoparticles and achieving uniform. Utilizing biological truths, like micro-organisms or plant extracts the synthesis practice, eco-friendly methods have been developed to overcome the challenges.<sup>[7]</sup> One of the biggest advantages of using plant materials for nanoparticle synthesis is that it eliminates the need for labor-intensive procedures like compound decontamination steps and maintaining microbial cell cultures.<sup>[8]</sup> The majority of the environmentally friendly methods reported have a number of problems, including stability, crystal growth, and particle aggregation.

Due to their well-known health advantages, silver utensils have been a standard item in the average household since the beginning of time. Due to the altered physical and chemical characteristics of silver and other metal nanoparticles, which can fight bacteria, they have been successfully and widely used in many industries, particularly in medicine.<sup>[9]</sup> Among different kinds of metals, SNPs have demonstrated a high potential for use in the pharmaceutical industry.<sup>[10]</sup> According to reports, SNPs have been used to make anti-infection creams and ointments for burns and wounds.<sup>[11]</sup> Additionally, they can be used as optical components, such as fluorescent probes and sensors for bioimaging.<sup>[12]</sup> This characteristic results from the distinctive optical, electrical, and catalytic characteristics of SNPs. Due to SNPs' distinctive application characteristics, including their anti-bacterial, anti-fungal,<sup>[13]</sup> anti-inflammatory,<sup>[14]</sup> anti-angiogenesis,<sup>[15]</sup> anti-viral, anti-platelet,<sup>[16]</sup> and other activities, biomedicine has made extensive use of them.<sup>[17]</sup> Because they are incredibly effective at stopping and killing bacteria, silver-based medicine products have actually been used for a very long time to prevent and treat a variety of diseases and infections. As a result, one of the most active research areas in recent years has been the production of silver nanoparticles. An emerging field of nanoscience research is the biosynthesis of nanoparticles. Compared to physical and chemical methods, these strategies have many benefits, such as being more affordable, requiring less energy, being more environmentally friendly, and being easier to use.<sup>[18]</sup> Plant-derived metal nanoparticles have completely changed the field of nanotechnology. Metal nanoparticles are synthesized environmentally friendly through the components of plant extracts. The chemical components help form stable nanoparticles by acting as a capping agent as well as a powerful reducing agent.<sup>[19]</sup>

*Afrohybanthus travancoricus* (Bedd.) Flicker is a member of the Violaceae family (Violet family). It consists of 150 species that are found into tropical, subtropical regions of the world, and are frequently seen in mountainous areas.<sup>[20]</sup> Travancore Green violet is a shrub that grows up to 1.75 m tall and has branches that are erect, round below, angled above, woody, and hairless. Leaves are alternate, nearly stalkless, linear-lance shaped, saw-toothed along

margins, tapering at tip, 1-9 x 0.5-2.5 cm, hairless; stipules are subulate, glandular-finely velvet-hairy. Flowers are produced in leaf axils on flower stalks that are 1-2 cm long and 2-bracteole towards the tip. Sepals are nearly equal in size, finely pointed, and recurved. Petals are pink and variable, with the lower petal being long-clawed and pouch-shaped. Others are sickle-shaped, with hairs on the upper two spurs. There are 5 stamens, with the anthers closest to the large petal having a round gibbous spur at the base. The ovary is 1-celled, with numerous ovules and a clavate, incurved style. Fruit is a capsule with 6-9 striped white seeds. The Travancore Green violet is only found in the Southern Western Ghats. Flowering season: July-September. The plant is used to treat inflammation, dysuria, urinary infections, diarrhoea, leucorrhoea, and male infertility. It is also employed as an anti-malarial, aphrodisiac, demulcent, tonic, diuretic, and anti-convulsant.<sup>[21]</sup> The plant is used to treat a variety of conditions, including breast tone, asthma, epilepsy, painful dysentery, vomiting, burning sensation, and blood issues.<sup>[22]</sup>

According to our knowledge and a review of the literature, no report is available on the biosynthesis with silver nanoparticles and characterization of UV, FTIR, XRD, SEM, and EDX analysis, *A. travancoricus* exhibits *in vitro* antioxidant, anti-inflammatory, and anti-diabetic properties.

## MATERIALS AND METHODS

### Collection of Plant Material and Authentication

Botanical Survey of India, Coimbatore, identified *A. travancoricus* leaves collected in the Mothiramalai, Kanyakumari district, Tamil Nadu, during the month of July-September, 2021. Mothiramalai, Kanyakumari district, Tamil Nadu, and India, Altitude is 105.15 m, Latitude are 8.5016504 and Longitude are 77.2992115. The leaves of *A. travancoricus* were then thoroughly washed three times with water, followed by a final time with distilled water. These leaves were then air dried before being ground into a fine powder with a pestle and mortar. Until extraction, a separate container was used to store the powdered material.

### Preparation of *A. travancoricus* leaf extract

100 mL of double-distilled water and 10 g of plant powder were weighed, combined, and then boiled for 15 min. Extract was created after the material was filtered through Whatman No. 1 filter paper. For upcoming research, the prepared extract was stored at 4°C.

### Silver nanoparticles synthesis using *A. travancoricus* leaf extract

The source of the silver was a 1 mM silver nitrate (AgNO<sub>3</sub>) solution in double distilled water. The silver nitrate and leaf extract were combined into a 9:1 ratio. The reaction the heated mixture below its boiling point and continuously stirred with a magnetic stirrer at 800 rpm. Within 24 hr in a dark room, the mixture had turned

reddish brown. Before being characterised, the nanoparticles were kept in an environment that was cool, dry, and dark.

### ATSNPs nanoparticles' characterization

#### Analysis using UV-visible spectroscopy

Using the Perkin-Elmer UV-vis Spectrometer Lambda-35, it is possible to observe how silver nanoparticles in the solution were being reduced. The solution was scanned at 480 nm/min in wavelength ranges from 100 to 400 nm at various reaction rates. The Spectrophotometer had "UV Win lab" software for recording and analyzing data. The baseline of the spectrometer was adjusted using a blank reference. *A. travancoricus* Silver Nanoparticles (ATSNPs) UV-vis absorption spectra and the resulting information were recorded in graphical form. The reaction solution was incubated for 24 hr to examine how time affected the formation of AgNPs.

#### Fourier Transform Infrared (FTIR) Measurement

In order to investigate and forecast any physicochemical interactions between various constituents in a formulation, FTIR measurements were carried out in the dried biomass of the extract treated with AgNO<sub>3</sub> in order to identify the compound responsible for the synthesis of ATSNPs. FTIR measurements were made on the synthesised SNPs 24 hr after the reaction began. The spectra were collected using samples that contained KBr pellets and an FTIR PERKIN ELMER instrument with a wavelength range of 4000 to 400 nm. The outcomes included comparisons of the functional peak shifts.

#### Analysis of X-ray Diffraction measurement (XRD)

The X-ray Diffraction (XRD) analysis was finished using RICA KU ULTIMA. The crystalline structure of the bio-synthesised silver nanoparticles was investigated using an X-ray powder diffracts metre and the X-ray diffraction technique. Using this technique, silver nanoparticles made by biological processes are examined for their crystalline structure. The silver nanoparticle dispersion was spread on a glass slide, and the ethanol solution was then allowed to evaporate, resulting in a thin film of silver and copper nanoparticles. With a 10-80 operating range and a 2θ/min scanning speed, this thin film was subjected to X-ray diffraction.

#### Analysis of Scanning Electron Microscopy (SEM)

Utilizing the QUANTO 250 scanning electron microscope, ATSNPs were examined using Scanning Electron Microscopy (SEM). Simply dropping the sample onto a copper grid that had been coated in carbon resulted in thin films. After blotting paper was used to remove excess solution from the films, the films on the SEM grid were given 5 min to dry under a mercury lamp.

### Energy Dispersive X-ray (EDX) Analysis

Silver elements were located and their presence was verified using EDX analysis. The configuration of the synthesised nanoparticles was then looked at after a very small amount of the sample ATSNPs were drop coated onto carbon film.<sup>[23]</sup>

### Activity of Antioxidant

#### DPPH (2, 2-diphenyl-1-picrylhydrazyl) Radical Scavenging method

The ATSNPs leaf extract was tested at various concentrations (100, 200, 300, 400, and 500 µg/mL) for its capacity to scavenge DPPH radicals.<sup>[24]</sup> A mixture of the test samples (between 100 and 500 mL), 0.8 mL of Tris-HCl buffer (pH 7.4), and 1 mL of DPPH was used (500 mM ethanol). The mixture was vigorously shaken before being set aside for 30 min. A UV-vis Spectrophotometer set to 517 nm was used to measure the solution's absorbance (UV-160A; Shimadzu Co.). The potential for radical scavenging was expressed as the concentration at which 50% of the DPPH radicals are scavenged, which is known as the IC<sub>50</sub> value. Using the following equation, the DPPH radical's scavenging activity was determined. Percentage inhibition is equal to (Acontrol-A sample) x 100. A control is the blank absorbance in cases where a sample is the DPPH solution's absorbance. Ascorbic acid, a synthetic antioxidant, served as a good control.

#### ABTS+ (2, 2'-azino-bis (3-ethylbenzothiazoline-6-sulfonic acid) Assay

Siddhuraju and Manian measured antioxidant activity using an improved ABTS+ method.<sup>[25]</sup> 2.45 mM potassium persulfate and 7 mM ABTS<sup>+</sup> were combined to create the radical, which was then left to sit at room temperature and in the dark for 12 to 16 hr. After that, ethanol was added to the solution to dilute it and create 734 nm absorbance. The diluted ABTS<sup>+</sup> solution and 10 mL of the ATSNPs sample were combined. After a 30 min incubation period, the absorbance was measured at 734 nm.

### Activity of Anti-inflammatory

#### Albumin denaturation inhibition

Plant extract have been tested for their ability to reduce inflammation using the inhibition of albumin denaturation technique.<sup>[26, 27]</sup>

### Chemical Reagents

- 1) 5% Bovine serum albumin.
- 2) 1N HCL.
- 3) Phosphate buffer saline.

### Procedure

5% bovine serum albumin and distilled water made up the reaction mixture (0.5 mL). 1 N HCl was used to raise the pH to 6.3. Various concentrations of plant extract were added to

the reaction mixture and heated for 5 min at 57°C after 20 min of incubation at 37°C. After the samples had cooled, 2.5 mL of phosphate buffer saline was added. Turbidity was determined spectrophotometrically at 600 nm. The formula below was used to calculate the percentage inhibition of protein denaturation:

$$\text{Percentage inhibition} = \frac{\text{Abs}_{\text{control}} - \text{Abs}_{\text{sample}}}{\text{Abs}_{\text{control}}} \times 100$$

## Antidiabetic activity

### $\alpha$ -Amylase inhibition assay<sup>[28]</sup>

#### Chemical Reagents

1. 0.02 M Sodium phosphate buffer (pH 6.9).
2. 0.006 M NaCl.
3. 1% Starch.
4. Dinitro salicylic acid.

#### Methods

500  $\mu$ L of 0.02 M sodium phosphate buffer (pH 6.9 with 0.006 M NaCl) and the porcine pancreatic  $\alpha$ -amylase enzyme (EC 3.2.1.1) were combined, and the mixture was then incubated at 25°C for 10 min. The reaction mixture was then given 500  $\mu$ L of a 1% starch solution in a 0.02 M sodium phosphate buffer (pH 6.9 with 0.006 M NaCl). After being incubated for 10 min at 25°C, the reaction mixture was then given a dose of Dinitrosalicylic Acid (DNSA). By incubating in boiling water and allowing to cool to room temperature, the reaction was stopped. A spectrophotometer was used to measure the absorbance at 540 nm after 10 mL of distilled water had been added.

$$\text{Percentage inhibition} = \frac{\text{Abs}_{\text{control}} - \text{Abs}_{\text{sample}}}{\text{Abs}_{\text{control}}} \times 100$$

The IC<sub>50</sub> value is the amount of sample extract that must be used in order to inhibit 50% of  $\alpha$ -amylase activity during an assay.

### $\alpha$ -Glucosidase inhibition assay<sup>[29]</sup>

#### Chemical Reagents

1.  $\alpha$ -glucosidase (0.5 mg/mL).
2. 0.1 M phosphate buffer (pH 6.9).
3. 5M p-nitrophenyl- $\alpha$ -D-glucopyranoside.

#### Procedure

200-1000 mg/mL of plant extract and 0.5 mg/mL of  $\alpha$ -glucosidase in 100 mL of 0.1 M phosphate buffer were incubated for 10 min at 25°C (pH 6.9). The mixture was then combined with 50  $\mu$ L of a 0.1 M phosphate buffer (pH 6.9) solution containing 5 M p-nitrophenyl-D-glucopyranoside before being allowed to cool to room temperature. Reaction mixtures were incubated for 5 min at 25°C, and then their absorbance at 405 nm was measured using a spectrophotometer. Without including the sample, all

other reagents and enzymes were combined to serve as controls, and the percentage of inhibition was calculated by contrasting it with the controls. To calculate the percentage of  $\alpha$ -glucosidase inhibitory activity, use the following formulas:

$$\text{Percentage inhibition} = \frac{\text{Abs}_{\text{control}} - \text{Abs}_{\text{sample}}}{\text{Abs}_{\text{control}}} \times 100$$

The IC<sub>50</sub> value is defined as the concentration of sample required to inhibit 50% of  $\alpha$ -glucosidase activity under assay conditions.

## RESULTS AND DISCUSSION

### Synthesis of silver nanoparticles

In this study, we used a green approach to synthesis ATSNPs leaf aqueous extract. The constituents of ATSNPs leaf aqueous extract reduced AgNO<sub>3</sub> with temperatures ranging from 60°C to 80°C and continuous stirring. SNPs were formed when the colour changed from light yellow to dark brown. Other researchers who used plant extracts as a reducing agent reported similar findings.<sup>[30]</sup> Figure 1 depicts the biological method used to synthesise silver nanoparticles by reducing AgNO<sub>3</sub> solution with plant extract. The brown colour in Figure 1 denoted the biological synthesis of silver nanoparticles. This result is similar with previous research,<sup>[31]</sup> which asserts that some secondary metabolites, such as polyphenols, alkaloids, terpenoids, proteins, and so on, have the ability to reduce silver ions when they are present in plant extracts.<sup>[32]</sup> The *A. travancoricus* Silver Nanoparticles (ATSNPs) were then created, centrifuged for 5 min at 4000 rpm, then poured into a petri dish and dried at 40°C on a hot plate. The powder is scratched with a clean blade before being stored in an eppendorff tube for further analysis.

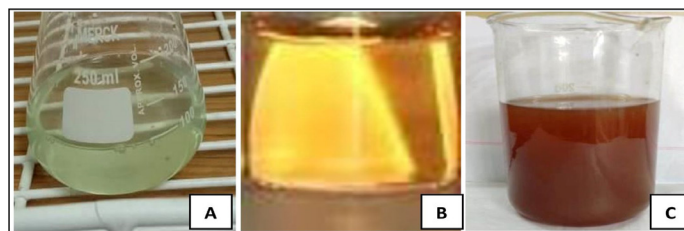


**Figure 1:** Synthesis of silver nanoparticles.

(A) 5mM AgNO<sub>3</sub> solution, (B) Plant extract and 5  $\mu$ m silver solution initial stage, (C) Bio-synthesized *A. travancoricus* silver nanoparticles.

### Analysis of UV-visible spectroscopy

The synthesized SNPs were mainly recognized by their UV-vis absorption spectrum, which is one of the most widely used techniques for analysing NPs. We evaluated the properties of the silver nanoparticles generated biologically using UV-visible spectroscopy. The peak between 290 and 350 nm (Figure 2) showed that silver ions were reduced, supporting the formation of silver nanoparticles produced through biological synthesis.<sup>[33]</sup>

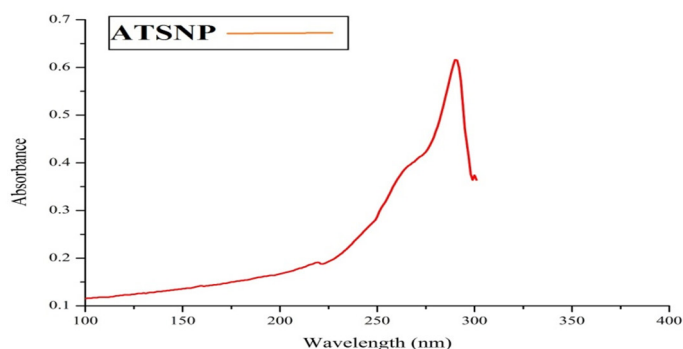


Figure 2: UV-visible spectroscopy analysis of ATSNPs.

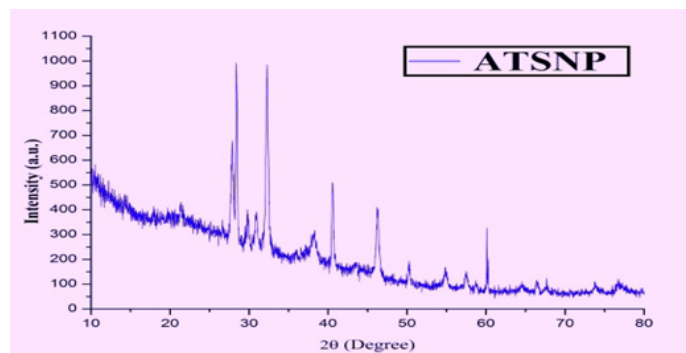


Figure 4: XRD analysis of ATSNPs.

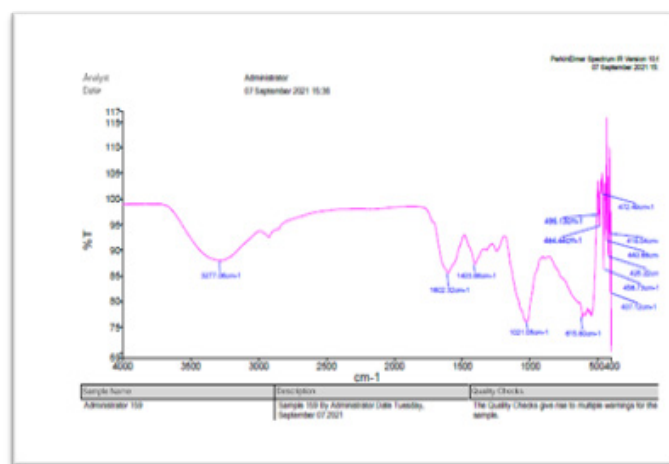


Figure 3: FT-IR peaks of ATSNPs.

This result coincides with *Ceropegia juncea*,<sup>[34]</sup> and *Pogostemon speciosus*.<sup>[35]</sup>

### FT-IR analysis

To determine the functional groups that are present in the ATSNPs, its FT-IR spectrum was analysed (Figure 3). Figure 3 displays to identify the various functional groups, FTIR spectrum is used that served as capping agents. 4000-400  $\text{cm}^{-1}$  is the typical IR absorption range. ATSNPs revealed 10 distinct peaks. The following measurements are in  $\text{cm}^{-1}$ : 3277.06  $\text{cm}^{-1}$ , 1602.32  $\text{cm}^{-1}$ , 1403.86  $\text{cm}^{-1}$ , 1021.05  $\text{cm}^{-1}$ , 615.80  $\text{cm}^{-1}$ , 496.13  $\text{cm}^{-1}$ , 484.44  $\text{cm}^{-1}$ , 472.49  $\text{cm}^{-1}$ , 458.73  $\text{cm}^{-1}$ , and 407.12  $\text{cm}^{-1}$  (Figure 3). Alkyl halides, alcohols, phenols, alkenes, alkanes, aliphatic amines, alkynes, alkanes, and aromatics are the functional groups, according to studies by Singh *et al.*<sup>[36]</sup> (Table 1). Based on the findings of the FT-IR analysis, a broad peak at 3277.06  $\text{cm}^{-1}$ , which is associated with O-H stretch alcohols and phenols, indicates a potent hydrogen bonding interaction between silver and the O-H groups. Peak at 1021.05  $\text{cm}^{-1}$ , which is in good agreement with the other reports, is related to C-N stretching and bending vibrations in amines from proteins, respectively.<sup>[37]</sup> Similar studies were reported in *Ceropegia juncea*,<sup>[34]</sup> and *Pogostemon speciosus*.<sup>[35]</sup> The synthesized nanoparticles' FTIR spectra, which concur with our

Table 1: FT-IR analysis of ATSNPs.

Sl. No.	Frequency Range	Bond	Functional Group
1.	3277.06 $\text{cm}^{-1}$	O-H stretch, H-bonded	Alcohols, phenols
2.	1602.32 $\text{cm}^{-1}$	-C=C- stretch	Alkenes
3.	1403.86 $\text{cm}^{-1}$	C-H bend	Alkanes
4.	1021.05 $\text{cm}^{-1}$	C-N stretch	aliphatic amines
5.	615.80 $\text{cm}^{-1}$	-C≡C-H: C-H bend	Alkynes
6.	496.13 $\text{cm}^{-1}$	C-Br stretch	Alkyl halides
7.	484.44 $\text{cm}^{-1}$	-C≡C-H: C-H bend	Alkynes
8.	472.49 $\text{cm}^{-1}$	C-H rock	Alkanes
9.	458.73 $\text{cm}^{-1}$	C-H "oop"	Aromatics
10.	407.12 $\text{cm}^{-1}$	C-Br stretch	Alkyl halides

EDX results, did not display a stretching band related to the Nitro Bond (N-O) at around 1280  $\text{cm}^{-1}$ , indicating that there were no nitrate traces that could be detected (where N was not observed). This demonstrates that the successful formation of AgNPs is due to the phytomolecules (secondary metabolites), which may serve as both reducing and capping agents.

### XRD analysis

The primary objective of the X-ray diffractometer experiment was to examine the crystalline makeup of the bio-synthesised ATSNPs and the  $2\theta$  values of the peaks with a range of  $0^\circ$  to  $80^\circ$ . The ATSNPs exhibit monocrystallinity, as can be seen in Figure 4. The XRD shows peaks at  $20.8^\circ$ ,  $30.3^\circ$ ,  $40.1^\circ$ ,  $40.9^\circ$ , and  $60^\circ$ , with  $20.8^\circ$  being the highest. These peaks can be indexed to the (111), (200), (220), and (622) planes, demonstrating the high degree of crystallinity of the ATSNPs. It is noteworthy that these four characteristic peaks represent the upper limit for highly pure SNPs.<sup>[35,37]</sup> This demonstrates that SNPs were successfully synthesised and establishes their crystalline nature.<sup>[38]</sup> SNPs that were made greenly using additional plant extracts showed comparable diffraction patterns.<sup>[31]</sup>

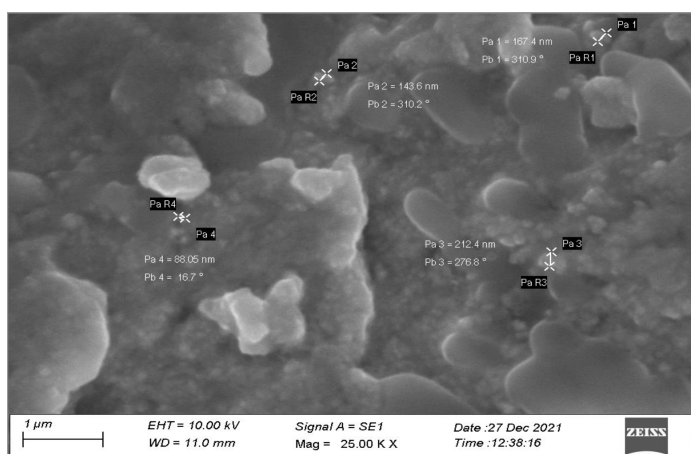


Figure 5: SEM analysis of ATSNPs.

## SEM analysis

SEM images of the ATSNPs are shown in Figure 5. SEM analysis of ATSNPs revealed the size and shape of the synthesised nanoparticles. The synthesised nanoparticles range in size from 88 nm to 242 nm (Figure 5). Similar results were also observed from *Ajuga bracteosa* and *Cinnamomum tamala* SNPs.<sup>[39,40]</sup> It is possible that the clustering of nanoparticles is caused by the interaction of concentrated nanoparticles with the organic components of *Bixa orellana* seed extracts used in biosynthesis.<sup>[41]</sup> This could be as a result of the ATSNPs' varied amounts and types of capping agents. The size of silver nanoparticles below 100 nm shows a wide range of applications for the synthesised nanomaterials, such as drug delivery, photochemical dye degradation, anti-cancer, antimicrobial, anti-inflammatory, antioxidant, and antidiabetic activities. Except for a few large aggregates, SEM images also showed crystalline and quasi-spherical shapes. The synthesised AgNPs in the colloidal solution may have a uniform spherical shape.<sup>[42]</sup>

## Analysis of EDX

The surface elemental composition of the biosynthesised nanomaterials was analysed using EDX spectroscopy. Typically, the SPR makes silver's optical absorption peak appear at 3 keV.<sup>[37]</sup> The silver atoms were the strongest signal, according to EDX analysis of the elemental composition (Figure 6). The analysis's findings suggested that the nanostructures were made entirely of silver. The silver nanoparticles created by ATSNPs amply demonstrate their nature as nanoparticles and support their environmentally friendly synthesis. The nanoparticles' silver atoms generated a potent EDX signal. Similar findings were reported in *Brassica oleracea* leaves extract of the SNPs,<sup>[43]</sup> and Ag was detected in the EDAX spectrum.<sup>[44]</sup>

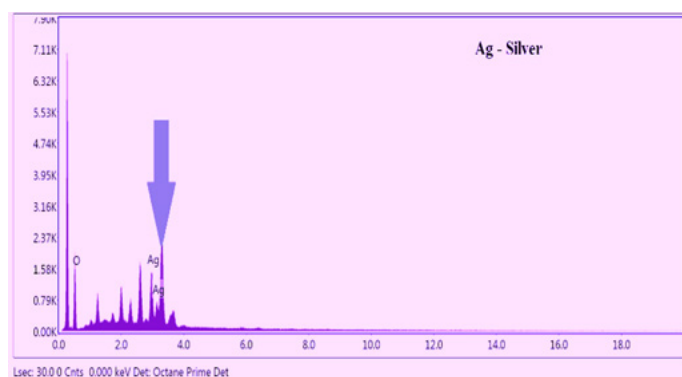


Figure 6: EDAX analysis of ATSNPs.

Table 2: DPPH assay of ATSNPs.

Sl. No.	Name of the assay	10 μg/mL	25 μg/mL	50 μg/mL	100 μg/mL	150 μg/mL	IC <sub>50</sub> μg/mL
1	DPPH assay	11.0	18.7	26.5	41.5	58.2	125
2	Ascorbic acid	31.94	41.69	51.09	61.15	65.33	115

## Antioxidant activity

### DPPH assay

Antioxidants, which can be natural or synthetic, are essential for preventing or delaying the cell damage brought on by oxidants.<sup>[37,45]</sup> Carbon nanotubes, metal and metal oxide nanoparticles, as well as other kinds of nanomaterials, have all been reported to possess antioxidant properties.<sup>[46]</sup> The ATSNPs were reacted to the DPPH's colour changing from dark purple to light purple. At higher concentrations, the percentage of inhibition was observed (Figure 7 and Table 2). At 150 μg/mL concentration, ATSNPs displayed the highest DPPH scavenging inhibition at 58.2%. SNPs in the stem bark extract of *Diospyros montana* yielded a similar report.<sup>[47]</sup> The second-highest inhibition 41.5%, at a concentration of 100 μg/mL. At 10 μg/mL concentration, the lowest percentage of inhibition was found to be 11.0% (Table 2). With a lowest IC<sub>50</sub> value of 125 μg/mL when compared to the ascorbic acid standard of 115 μg/mL, ATSNPs has the potential to scavenge DPPH. With an IC<sub>50</sub> value of 30.04 μg/mL in earlier studies, SNPs in *Erythrina suberosa* leaf extract demonstrated good DPPH activity.<sup>[48]</sup>

### ABTS<sup>+</sup> assay

The percentage inhibition of free radicals was used to assess the ATSNPs' ability to scavenge ABTS<sup>+</sup> radicals. ATSNPs were found to have the highest ABTS<sup>+</sup> radical scavenging percentage, with 52.6% at a concentration of 150 μg/mL (Figure 8 and Table 3). The lowest IC<sub>50</sub> value for ATSNPs was 143 μg/mL, which is roughly equivalent to the ascorbic acid concentration of 125 μg/mL. ATSNPs were found to have the second-highest

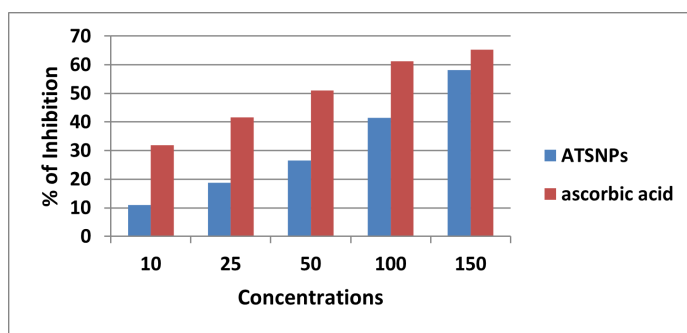


Figure 7: DPPH assay of ATSNPs.

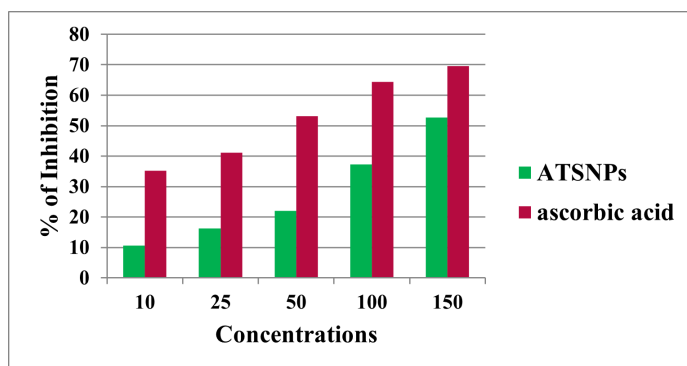


Figure 8: ABTS+ assay of ATSNPs.

Table 3: ABTS+ assay of ATSNPs

Sl. No.	Name of the assay	10 µg/mL	25 µg/mL	50 µg/mL	100 µg/mL	150 µg/mL	IC <sub>50</sub> µg/mL
1	ABTS+ assay	10.6	16.3	22.0	37.2	52.6	143
2	Ascorbic acid	35.14	41.09	53.18	64.37	69.48	125

percentage inhibition (37.2%) at a concentration of 100 µg/mL. Recent research using various plant extract and green synthesis of SNPs revealed significant ABTS+ activities.<sup>[34]</sup> Standard ascorbic acid has an IC<sub>50</sub> value of 125 µg/mL (Table 3). An earlier study found that SNPs in *Cassia angustifolia* flower extract had an IC<sub>50</sub> value of 78.10 µg/mL.<sup>[49]</sup>

### In vitro Anti-inflammatory activity

#### Albumin denaturation assay

Protein denaturation is one of the well-known causes of inflammatory and arthritic diseases.<sup>[50]</sup> According to reports, the production of autoantigens in some types of arthritic diseases may be caused by the *in vivo* denaturation of tissue proteins.<sup>[51]</sup> The anti-inflammatory activity of the extract was examined by testing the nanoparticles' capacity to prevent protein denaturation through inhibition of the egg albumin denaturation assay. Table 4 lists the concentrations of the ATSNPs that were most effective at

Table 4: Albumin denaturation assay of ATSNPs.

Sl. No.	Concentration µg/mL	Percentage inhibition	
		Albumin denaturation	Aspirin
1	10	11.6	30.49
2	25	20.2	44.22
3	50	31.4	56.15
4	100	50.0	64.53
5	150	68.7	83.38

IC<sub>50</sub> value of ATSNPs = 101 µg/mL; IC<sub>50</sub> value of Aspirin = 42 µg/mL.

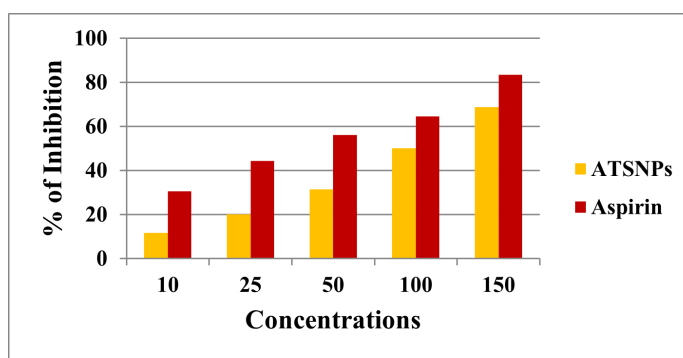


Figure 9: Albumin denaturation assay of ATSNPs.

preventing heat-induced albumin denaturation. When calculating the percentage of inhibition, ATSNP concentrations between 10 and 150 µg/mL were used. From lowest concentration (10 µg/mL) to highest concentration (150 µg/mL) of ATSNPs, respectively, the percentage inhibition ranged from 11.6, 20.2, 31.4, 50.0, and 68.7 (Figure 9). In a related study, zinc oxide nanoparticles made from grape seed extract displayed the highest absorbance value at a concentration of 50 µL.<sup>[52]</sup> The 50% inhibition (IC<sub>50</sub>) concentration of ATSNPs was observed at 101 µg/mL, whereas the IC<sub>50</sub> value for the control drug aspirin was 42 µg/mL. We can infer from a study that silver, when compared to any anti-inflammatory drug, can produce powerful anti-inflammatory activity.<sup>[35]</sup>

### In vitro Antidiabetic activity

#### α-Amylase activity

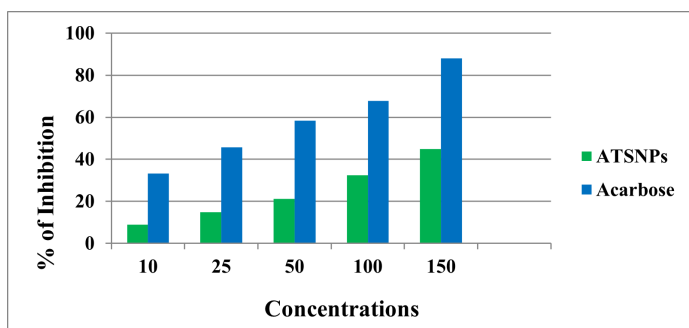
The synthesized compounds came in five different concentrations (10, 25, 50, 100, and 150 µg/mL, respectively) ATSNPs' dose-dependent antidiabetic activity increased in percentage inhibitory activity against the α-amylase enzyme, with inhibition percentages of 9.0%, 14.8%, 21.2%, 32.5%, and 44.8% (Table 5). SNPs were produced using *Tephrosia tinctoria* stem extract and *Calophyllum tomentosum* leaf extract, and the outcomes showed activity to inhibit α-Amylase. Studying the silver nanoparticles from *Allium cepa* for their *in vitro* anti-diabetic properties revealed that the particles have higher levels of α-amylase

**Table 5:  $\alpha$ -Amylase activity of ATSNPs.**

Sl. No.	Name of the assay	10 $\mu\text{g}/\text{mL}$	25 $\mu\text{g}/\text{mL}$	50 $\mu\text{g}/\text{mL}$	100 $\mu\text{g}/\text{mL}$	150 $\mu\text{g}/\text{mL}$	$\text{IC}_{50}$ $\mu\text{g}/\text{mL}$
1	$\alpha$ – Amylase activity	9.0	14.8	21.2	32.5	44.8	170
2	Acarbose	33.19	45.76	58.34	67.75	88.12	125

**Table 6:  $\alpha$ -Glycosidase activity of ATSNPs.**

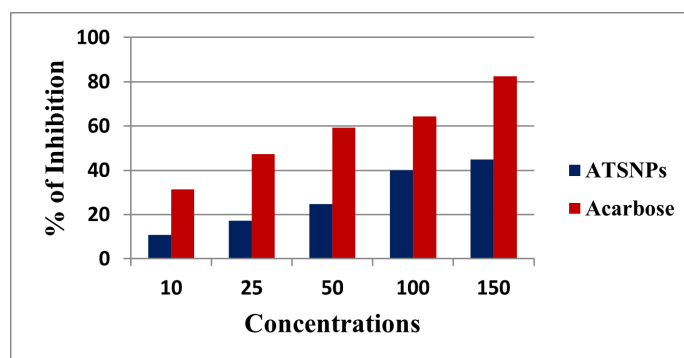
Sl. No.	Name of the assay	10 $\mu\text{g}/\text{mL}$	25 $\mu\text{g}/\text{mL}$	50 $\mu\text{g}/\text{mL}$	100 $\mu\text{g}/\text{mL}$	150 $\mu\text{g}/\text{mL}$	$\text{IC}_{50}$ $\mu\text{g}/\text{mL}$
1	$\alpha$ – Glycosidase activity	10.7	17.2	24.8	40.1	54.4	134
2	Acarbose	31.37	47.26	59.26	64.38	82.47	127

**Figure 10:  $\alpha$ -Amylase activity of ATSNPs.**

and  $\alpha$ -glucosidase activities.<sup>[53]</sup> The  $\text{IC}_{50}$  value for this assay is 170  $\mu\text{g}/\text{mL}$  (Table 5), and the best rate of inhibition was observed at 150  $\mu\text{g}/\text{mL}$ , followed by 100  $\mu\text{g}/\text{mL}$  (Figure 10). Vishnu and Murugesan,<sup>[54]</sup> used silver nanoparticles made from *Halymenia poryphyroides* and came to similar conclusions. With an increase in percentage  $\alpha$ -amylase inhibitory activity, these nanoparticles showed remarkable dose-dependent *in vitro* antidiabetes effectiveness. Similar  $\alpha$ -amylase inhibition activity was also seen in the silver nanoparticles made from other medicinal plants.<sup>[55]</sup>

### $\alpha$ -Glycosidase activity

By catalyzing the conversion of oligosaccharides and disaccharides into monosaccharides,  $\alpha$ -glucosidase is another important enzyme in the metabolism of carbohydrates.<sup>[56]</sup> Studies have shown that inhibiting  $\alpha$ -glucosidase can prevent the digestion and absorption of carbohydrates, which lowers blood sugar levels.<sup>[57]</sup> The enzyme activity of the ATSNPs extract  $\alpha$ -Glucosidase was tested in the current study. The extract results are shown in Table 6, which demonstrates that as concentration increases;  $\alpha$ -Glucosidase enzyme activity is also inhibited more frequently. At a concentration of 150  $\mu\text{g}/\text{mL}$  of ATSNPs extract,

**Figure 11:  $\alpha$ -Glycosidase activity of ATSNPs.**

the observed inhibition percentage was 54.4. When compared to the control substance acarbose, the extract has the highest percentage of inhibition activity at a concentration of 150  $\mu\text{g}/\text{mL}$ , with a value of 82.47 (Figure 11). Acarbose served as the control and had an  $\text{IC}_{50}$  value of 127  $\mu\text{g}/\text{mL}$ , while-glycosidase inhibition activity had an  $\text{IC}_{50}$  value of 134  $\mu\text{g}/\text{mL}$  (Table 6). Similar results were also seen with the green silver nanoparticles derived from other medicinal plants.<sup>[58]</sup>

## CONCLUSION

The current study demonstrates the quick, easy, and affordable synthesis of SNPs in an eco-friendly manner using the aqueous leaf extract of the medicinal plant *A. travancoricus*. There is no report on the synthesis of nanoparticles using *A. travancoricus*, despite the fact that researchers in this field have conducted numerous studies on a variety of medicinal plants. In order to assess its potential for use in *in vitro* biomedical applications, an effort was made to synthesise SNPs through *A. travancoricus*-mediated synthesis. Biosynthesized AgNPs demonstrated notable antioxidant, anti-inflammatory, and antidiabetic effects. The successful formation of spherical and crystalline SNPs was confirmed by several physico-chemical characterization techniques, which also provided proof that the phytochemicals in the extract functioned as reducing and capping agents in the green synthesis of SNPs. SNPs also demonstrated potent antioxidant, anti-inflammatory, and antidiabetic properties in the biological analysis. Additional investigation is necessary to confirm the precise mechanism of action of this product in animal and human samples before it can be suggested as a pharmacological agent for the treatment of oxidative stress, inflammation, and diabetes.

## CONFLICT OF INTEREST

The authors declare that there is no conflict of interest.

## ABBREVIATIONS

**ATSNPs:** *Afrohybanthus travancoricus* silver nanoparticles; **FT-IR:** Fourier transform infrared spectroscopy; **XRD:** X-ray powder diffraction analysis; **SEM:** Scanning electron microscope; **EDX:** Energy dispersive X-ray analysis; **AgNO<sub>3</sub>:** Silver nitrate;

**DPPH:** 2,2-diphenylpicrylhydrazyl assay; **ABTS:** 2,2'-azino-bis(3-ethylbenzothiazoline-6-sulfonic acid) assay; **IC<sub>50</sub>:** Fifty percent of inhibition concentration.

## AUTHORS' CONTRIBUTIONS

Balrajmani Davidson Raja- developed the concept, did the experiments, generated and analyzed the data, guarantor. Devaraj Sathiya Sheela- provide literature review, data analysis. Elumalai Shanthi Priya- reviewed the concept, experimental design, and literature. Ammasaikutty Vanitha- prepared the first draft of this manuscript, literature search, data collection, analysis and statistics, updating and editing, guarantor. Kandasamy Kalimuthu- manuscript review, organization and analysis, guarantor. Periannan Viswanathan- detailed review of the manuscript, supervised the day-to-day experiments of the project, guarantor. All authors contributed to the final version of the manuscript.

## REFERENCES

- Nagajyothi PC, Cha SJ, Yang JJ, Sreekanth TVM, Kim KJ, Shin HM. Antioxidant and anti-inflammatory activities of zinc oxide nanoparticles synthesized using *Polygala tenuifolia* root extract. *J Photochem Photobiol B*. 2015;146:10-7. doi: 10.1016/j.jphotobiol.2015.02.008, PMID 25777265.
- Nazeruddin GM, Prasad NR, Waghmare SR, Garadkar KM, Mulla IS. Extracellular biosynthesis of silver nanoparticle using *Azadirachta indica* leaf extract and its antimicrobial activity. *J Alloys Compd*. 2014;583:272-7. doi: 10.1016/j.jallcom.2013.07.111.
- Chaudhry Q, Castle L. Food applications of nanotechnologies: an overview of opportunities and challenges for developing countries. *Trends Food Sci Technol*. 2011;22(11):595-603. doi: 10.1016/j.tifs.2011.01.001.
- Pu HL, Chiang WL, Maiti B, Liao ZX, Ho YC, Shim MS, et al. Nanoparticles with dual responses to oxidative stress and reduced pH for drug release and anti-inflammatory applications. *ACS Nano*. 2014;8(2):1213-21. doi: 10.1021/nn4058787, PMID 24386907.
- Mukunthan KS, Elumalai EK, Patel TN, Murty VR. *Catharanthus roseus*: a natural source for the synthesis of silver nanoparticles. *Asian Pac J Trop Biomed*. 2011;1(4):270-4. doi: 10.1016/S2221-1691(11)60041-5, PMID 23569773.
- Sharma VK, Yngard RA, Lin Y. Silver nanoparticles: green synthesis and their antimicrobial activities. *Adv Colloid Interface Sci*. 2009;145(1-2):83-96. doi: 10.1016/j.cis.2008.09.002, PMID 18945421.
- Saifuddin N, Wong CW, Yasumira AAN. Rapid biosynthesis of silver nanoparticles using culture supernatant of bacteria with microwave irradiation. *E-Journal of Chemistry*. 2009;6(1):61-70. ISSN: 0973-4945. doi: 10.1155/2009/734264.
- Narayanan KB, Sakthivel N. Green synthesis of biogenic metal nanoparticles by terrestrial and aquatic phototrophic and heterotrophic eukaryotes and biocompatible agents. *Adv Colloid Interface Sci*. 2011;169(2):59-79. doi: 10.1016/j.cis.2011.08.004, PMID 21981929.
- Kłębowski B, Depciuch J, Parlińska-Wojtan M, Baran J. Applications of noble metal-based nanoparticles in medicine. *Int J Mol Sci*. 2018;19(12). doi: 10.3390/ijms19124031, PMID 30551592.
- Nayak D, Pradhan S, Ashe S, Rauta PR, Nayak B. Biologically synthesized silver nanoparticles from three diverse family of plant extracts and their anti-cancer activity against epidermoid A431 carcinoma. *J Colloid Interface Sci*. 2015;457:329-38. doi: 10.1016/j.jcis.2015.07.012, PMID 26196716.
- Zhang XF, Choi YJ, Han JW, Kim E, Park JH, Gurunathan S, et al. Differential nanoreprotoxicity of silver nanoparticles in male somatic cells and spermatogonial stem cells. *Int J Nanomedicine*. 2015;10:1335-57. doi: 10.2147/IJN.S76062, PMID 25733828.
- Zhang LB, Wang EK. Metal nanoclusters: new fluorescent probes for sensors and bioimaging. *Nano Today*. 2014;9(1):132-57. doi: 10.1016/j.nantod.2014.02.010.
- Medina-Ramirez IM, Bashir S, Luo Z, Liu JL. Green synthesis and characterization of polymer-stabilized silver nanoparticles. *Colloids Surf B Biointerfaces*. 2009;73(2):185-91. doi: 10.1016/j.colsurfb.2009.05.015, PMID 19539451.
- Panáček A, Kolář M, Večeřová R, Pruček R, Soukupová J, Kryžof V, et al. Antifungal activity of silver nanoparticles against *Candida* spp. *Biomaterials*. 2009;30(31):6333-40. doi: 10.1016/j.biomaterials.2009.07.065, PMID 19698988.
- Rogers JV, Parkinson CV, Choi YW, Speshock JL, Hussain SM. A preliminary assessment of silver nanoparticle inhibition of monkeypox virus plaque formation. *Nanoscale Res Lett*. 2008;3(4):129-33. doi: 10.1007/s11671-008-9128-2.
- Nadworny PL, Wang J, Tredget EE, Burrell RE. Anti-inflammatory activity of nanocrystalline silver in a porcine contact dermatitis model. *Nanomedicine*. 2008;4(3):241-51. doi: 10.1016/j.nano.2008.04.006, PMID 18550449.
- Gurunathan S, Kalishwaralal K, Vaidyanathan R, Deepak V, Pandian SRK, Muniyandi J, et al. Biosynthesis, purification and characterization of silver nanoparticles using *Escherichia coli*. *Colloids Surf B Biointerfaces*. 2009; B;74(1):328-35. doi: 10.1016/j.colsurfb.2009.07.048, PMID 19716685.
- Gholami-Shabani M, Akbarzadeh A, Norouzi D, Amini A, Gholami-Shabani Z, Imani A, et al. Antimicrobial activity and physical characterization of silver nanoparticles green synthesized using nitrate reductase from *Fusarium oxysporum*. *Appl Biochem Biotechnol*. 2014;172(8):4084-98. doi: 10.1007/s12010-014-0809-2, PMID 24610039.
- Ansari MA, Khan HM, Khan AA, Cameotra SS, Alzohairy MA. Anti-biofilm efficacy of silver nanoparticles against MRSA and MRSE isolated from wounds in a tertiary care hospital. *Indian J Med Microbiol*. 2015;33(1):101-9. doi: 10.4103/0255-0857.148402, PMID 25560011.
- Amutha Priya D, Ranganayaki S, Suganya Devi P. Phytochemical screening and antioxidant potential of *Hybanthus enneaspermus*: A rare ethano botanical herb. *J Pharm Res*. 2011;4.
- Wahlert GA, Marcussen T, de Paula-Souza J, Feng M, Ballard HE. A phylogeny of the Violaceae (*Malpighiales*) inferred from plastid DNA sequences: implications for generic diversity and intrafamilial classification. *Syst Bot*. 2014;39(1):239-52. doi: 10.1600/036364414X678008.
- Awobajo FO, Olatunji-Bello II, Adegoke OA, Odugbemi TO. Phytochemical and antimicrobial screening of *Hybanthus enneaspermus* and *Paquetinagriscense*. *Recent Res Sci Technol*. 2009;1:159-60.
- Vigneshwaran N, Ashtaputre NM, Varadarajan PV, Nachane RP, Paralikar KM, Balasubramanya RH. Biological synthesis of silver nanoparticles using the fungus *Aspergillus flavus*. *Mater Lett*. 2007;61(6):1413-8. doi: 10.1016/j.matlet.2006.07.042.
- Kulkarni AP, Aradhya SM, Divakar S. Isolation and identification of anradical scavenging antioxidant-punicalagin from pith and carpellary membrane of pomegranate fruit. *Food Chem*. 2004;87(4):551-7. doi: 10.1016/j.foodchem.2004.01.006.
- Siddhuraju P, Manian S. The antioxidant activity and free radical-scavenging capacity of dietary phenolic extracts from horse gram (*Macrotyloma uniflorum* (Lam.) Verdc.) seeds. *Food Chem*. 2007;105(3):950-8. doi: 10.1016/j.foodchem.2007.04.040.
- Mizushima Y, Kobayashi M. Interaction of anti-inflammatory drugs with serum proteins, especially with some biologically active proteins. *J Pharm Pharmacol*. 1968;20(3):169-73. doi: 10.1111/j.2042-7158.1968.tb09718.x, PMID 4385045.
- Sakat S, Juvekar AR, Gambhire MN. *In vitro* antioxidant and anti-inflammatory activity of methanol extract of *Oxalis corniculata* Linn. *Int J Pharm Pharm Sci*. 2010;2:146-55. doi: 10.1055/s-0029-1234983.
- Worthington V. Alpha-amylase. In: Worthington V, editor. *Worthington enzyme manual freehold*. NJ: Worthington Biochemical Corp; 1993. p. 36-41.
- Apostolidis E, Kwon Y-I, Shetty K. Inhibitory potential of herb, fruit, and fungal enriched cheese against key enzymes linked to type 2 diabetes and hypertension. *Innov Food Sci Emerg Technol*. 2007;8(1):46-54. doi: 10.1016/j.ifset.2006.06.001.
- Jayapriya M, Dhanasekaran D, Arulmozhi M, Nandhakumar E, Senthilkumar N, Sureshkumar K. Green synthesis of silver nanoparticles using *Piper longum* catkin extract irradiated by sunlight: antibacterial and catalytic activity. *Res Chem Intermed*. 2019;45(6):3617-31. doi: 10.1007/s1164-019-03812-5.
- Oliveira GZS, Lopes CAP, Sousa MH, Silva LP. Synthesis of silver nanoparticles using aqueous extracts of *Pterodon emarginatus* leaves collected in the summer and winter seasons. *Int Nano Lett*. 2019;9(2):109-17. doi: 10.1007/s40089-019-0265-7.
- Kambale EK, Nkanga CI, Mutonkole BI, Bapolisi AM, Tassa DO, Liesse JI, et al. Green synthesis of antimicrobial silver nanoparticles using aqueous leaf extracts from three Congolese plant species (*Brillantaisia patula*, *Crossopteryx febrifuga* and *Sennasiamea*). *Heliyon*. 2020;6(8):e04493. doi: 10.1016/j.heliyon.2020.e04493, PMID 32793824.
- Kumar SV, Bafana AP, Pawar P, Rahman A, Dahoumane SA, Jeffryes CS. High conversion synthesis of <10 nm starch-stabilized silver nanoparticles using microwave technology. *Sci Rep*. 2018;8(1):5106. doi: 10.1038/s41598-018-23480-6, PMID 29572495.
- Subramaniam P, Vanitha A, Kalimuthu K, Sathiya Sheela D, Shanthi Priya E. Phytosynthesis of copper nanoparticles using wild *Ceropegia juncea* and its therapeutic activities. *Res. Jr Agril. Sci* 2022;13:1024-31.
- Sathiya Sheela D, Viswanathan P, Kalimuthu K, Vanitha A. Facile synthesis of silver nanoparticles, anti-inflammatory, antibacterial and photocatalytic activities using *Pogostemon speciosus* Benth. An endemic medicinal plant. *J Water Environ Nanotechnol*. 2022;7:306-16. doi: 10.22090/JWENT.2022.03.006.
- Singh H, Du J, Singh P, Yi TH. Ecofriendly synthesis of silver and gold nanoparticles by *Euphrasia officinalis* leaf extract and its biomedical applications. *Artif Cells Nanomed Biotechnol*. 2018;46(6):1163-70. doi: 10.1080/21691401.2017.1362417, PMID 28784039.
- Kingslin A, Kalimuthu K, Kiruthika ML, Khalifa AS, Nhat PT, Brindhadevi K. Synthesis, characterization and biological potential of silver nanoparticles using *Enteromorpha prolifera* algal extract. *Appl Nanosci*. 2022;1-14. doi: 10.1007/s13204-021-02105-x.
- Rónavári A, Kovács D, Igaz N, Vágvölgyi C, Boros IM, Kónya Z, et al. Biological activity of green-synthesized silver nanoparticles depends on the applied natural extracts:

- a comprehensive study. *Int J Nanomedicine*. 2017;12:871-83. doi: 10.2147/IJN.S122842, PMID 28184158.
39. Afreen A, Ahmed R, Mehboob S, Tariq M, Alghamdi HA, Zahid AA, et al. Phytochemical-assisted biosynthesis of silver nanoparticles from *Ajuga reptans* for biomedical applications. *Mater Res Express*. 2020;7(7):075404. doi: 10.1088/2053-1591/aba5d0.
  40. Nahar K, Aziz S, Bashir M, Haque M, Al-Reza SM. Synthesis and characterization of silver nanoparticles from *Cinnamom umtamala* leaf extract and its antibacterial potential. *Int J Nano Dimens*. 2020;11(1):88-98.
  41. Ssekatawa K, Byarugaba DK, Kato CD, Wampande EM, Ejobi F, Nakavuma JL, et al. Green strategy-based synthesis of silver nanoparticles for antibacterial applications. *Front Nanotechnol*. 2021;3:697303. doi: 10.3389/fnano.2021.697303.
  42. JerunNisha KM, Vanitha A, Kiruthika ML, Viswanathan P, Kalimuthu K. Biosynthesis of silver and copper nanoparticles using *Cadaba fruticosa* (L.) Druce and its biological applications. *Asian Pac. J Health Sci*. 2021;8:1-12. doi: 10.21276/apjhs.2021.8.3.12.
  43. Thi Lan Huong VTL, Nguyen NT. Green synthesis, characterization and antibacterial activity of silver nanoparticles using *Sapindus mukorossi* fruit pericarp extract. *Mater Today Proc*. 2021;42:88-93. doi: 10.1016/j.matpr.2020.10.015.
  44. Senthil-Nathan S. A review of resistance mechanisms of synthetic insecticides and botanicals, phytochemicals and essential oils as alternative larvicidal agents against mosquitoes. *Front Physiol*. 2019;10:1591. doi: 10.3389/fphys.2019.01591, PMID 32158396.
  45. Bedlovičová Z, Strapáč I, Baláz M, Salayová AA. A Brief overview on antioxidant activity determination of silver nanoparticles. *Molecules*. 2020;25(14):3191. doi: 10.3390/molecules25143191, PMID 32668682.
  46. Valgimigli L, Baschieri A, Amorati R. Antioxidant activity of nanomaterials. *J Mater Chem B*. 2018;6(14):2036-51. doi: 10.1039/C8TB00107C, PMID 32254427.
  47. Bharathi D, Diviya Josebin M, Vasantharaj S, Bhuvaneshwari V. Biosynthesis of silver nanoparticles using stem bark extracts of *Diospyros montana* and their antioxidant and antibacterial activities. *J Nanostruct Chem*. 2018;8(1):83-92. doi: 10.1007/s40097-018-0256-7.
  48. Mohanta YK, Panda SK, Jayabalan R, Sharma N, Bastia AK, Mohanta TK. Antimicrobial, antioxidant and cytotoxic activity of silver nanoparticles synthesized by leaf extract of *Erythrina suberosa* (Roxb.). *Front Mol Biosci*. 2017;4:14. doi: 10.3389/fmolb.2017.00014, PMID 28367437.
  49. Bharathi D, Bhuvaneshwari V. Evaluation of the cytotoxic and antioxidant activity of phyto-synthesized silver nanoparticles using *Cassia angustifolia* flowers. *BioNanoSci*. 2019;9(1):155-63. doi: 10.1007/s12668-018-0577-5.
  50. Shamsi TN, Parveen R, Afreen S, Azam M, Sen P, Sharma Y, et al. Trypsin inhibitors from *Cajanus cajan* and *Phaseolus limensis* possess antioxidant, anti-inflammatory, and antibacterial activity. *J Diet Suppl*. 2018;15(6):939-50. doi: 10.1080/19390211.2017.1407383, PMID 29345972.
  51. Umapathy E, Ndebia EJ, Meeme A. An experimental evaluation of *Albica setosa* aqueous extract on membrane stabilization, protein denaturation and white blood cell migration during acute inflammation. *J Med Plants Res*. 2010;4:9:789-95. doi: 10.5897/JMPR10.056.
  52. Agarwal H, Shanmugam V. A review on anti-inflammatory activity of green synthesized zinc oxide nanoparticle: mechanism-based approach. *Bioorg Chem*. 2020;94:103423. doi: 10.1016/j.bioorg.2019.103423, PMID 31776035.
  53. Jini D, Sharmila S. Green synthesis of silver nanoparticles from *Allium cepa* and its *in vitro* antidiabetic activity. *Mater Today Proc*. 2020;22:432-8. doi: 10.1016/j.bioorg.2019.103423.
  54. Vishnu K, Murugesan MS. Biogenic silver nanoparticles by *Halymenia poryphyroides* and its *in vitro* antidiabetic efficacy. *J Chem Pharm Res*. 2013;5(12):1001-8.
  55. Deepak P, Amutha V, Birundha R, Sowmiya R, Kamaraj C, Balasubramanian V, et al. Facile green synthesis of nanoparticles from brown seaweed *Sargassum wightii* and its biological application potential. *Adv Nat Sci Nanosci Nanotechnol*. 2018;9(3):10. doi: 10.1088/2043-6254/aadc4a.
  56. Chen G, Guo M. Rapid screening for  $\alpha$ -glucosidase inhibitors from *Gymnema sylvestris* by affinity ultrafiltration-HPLC-MS. *Front Pharmacol*. 2017;8:228. doi: 10.3389/fphar.2017.00228, PMID 28496409.
  57. Zhou X, Liang J, Zhang Y, Zhao H, Guo Y, Shi S. Separation and purification of  $\alpha$ -glucosidase inhibitors from *Polygonatum odoratum* by stepwise high-speed counter-current chromatography combined with Sephadex LH-20 chromatography target-guided by ultrafiltration-HPLC screening. *J Chromatogr B Analyt Technol Biomed Life Sci*. 2015;985:149-54. doi: 10.1016/j.jchromb.2015.01.030, PMID 25682336.
  58. Malapermal V, Botha I, Krishna SBN, Mbatha JN. Enhancing antidiabetic and antimicrobial performance of *Ocimum basilicum*, and *Ocimum sanctum* (L.) using silver nanoparticles. *Saudi J Biol Sci*. 2017;24(6):1294-305. doi: 10.1016/j.sjbs.2015.06.026, PMID 28855825.

**Cite this article:** Raja BD, Sheela DS, Priya ES, Vanitha A, Kalimuthu K, Viswanathan P. Phyto-mediated Synthesis of Silver Nanoparticles with *Afrohybanthus travancoricus* Leaf Aqueous Extract and Screening of their *in vitro* Antioxidant, Anti-Inflammatory, and Anti-diabetic Activities. *Pharmacog Res*. 2023;15(4):751-60.